
Hierarchical Graph Matching Networks for Deep Graph Similarity Learning

Xiang Ling^{1*} Lingfei Wu^{2*} Saizhuo Wang¹ Tengfei Ma² Fangli Xu³
 Alex X. Liu⁴ Chunming Wu¹ Shouling Ji^{1†}

¹Zhejiang University ²IBM Research ³Squirrel AI Learning ⁴Ant Financial Services Group

Abstract

While the celebrated graph neural networks yield effective representations for individual nodes of a graph, there has been relatively less success in extending to deep graph similarity learning. Recent work has considered either global-level graph-graph interactions or low-level node-node interactions, ignoring the rich cross-level interactions (*e.g.*, between nodes and a whole graph). In this paper, we propose a Hierarchical Graph Matching Network (HGMM) for computing the graph similarity between any pair of graph-structured objects. Our model jointly learns graph representations and a graph matching metric function for computing graph similarities in an end-to-end fashion. The proposed HGMM model consists of a node-graph matching network for effectively learning cross-level interactions between nodes of a graph and a whole graph, and a siamese graph neural network for learning global-level interactions between two graphs. Our comprehensive experiments demonstrate that HGMM consistently outperforms state-of-the-art graph matching network baselines for both classification and regression tasks.

1 Introduction

Learning a general similarity metric between arbitrary pairs of graph-structured objects is one of the key challenges in machine learning. Such learning problems arise in a variety of applications, ranging from graph searching in graph-based databases [43], to fewshot 3D action recognition [15] and malware detection [37]. Conceptually, classical exact or inexact graph matching techniques [9, 10, 32] provide a strong tool for learning graph similarity. However, these methods usually either require input graphs with similar sizes or consider mainly the graph structures for finding a correspondence between the nodes of different graphs without taking into account the node representations or features. In contrast, in this paper, we consider the graph matching problem of learning a mapping between a pair of graph inputs $(G^1, G^2) \in \mathcal{G} \times \mathcal{G}$ and the similarity score $y \in \mathcal{Y}$, based on a set of training triplet of graph input pairs and scalar output score $(G_1^1, G_1^2, y_1), \dots, (G_n^1, G_n^2, y_n) \in \mathcal{G} \times \mathcal{G} \times \mathcal{Y}$ drawn from some fixed but unknown probability distribution in real applications.

Although graph neural networks (GNNs) have recently demonstrated to be a powerful class of neural networks for learning node embeddings of graphs on tasks ranging from node classifications, graph classifications to graph generations [7, 25, 22, 16, 36], there is relatively less study on learning graph similarity using GNNs. A simple yet straightforward way is to use GNN to encode each graph as a vector and combine the vectors of two graphs to make a decision. This simple approach can be effective as the graph-level vector contains important information of a pair of graphs, but one obvious limitation is that this approach ignores finer-grained interactions among different-level embeddings of two graphs. Very recently, a few attempts have been made to take into account low-level interactions

*Both authors contributed equally to this research.

†Corresponding author.

either by considering the histogram information or spatial patterns (with CNNs) of the node-wise similarity matrix of node embeddings [1, 2], or by improving the node embeddings of one graph by incorporating the implicit attentive neighbors of another graph [24]. However, there are two significant challenges making these graph matching networks potentially ineffective: i) how to learn different-level granularity (global level and local level) of interactions between a pair of graphs; ii) how to effectively learn richer cross-level interactions between nodes of a graph and a whole graph.

Inspired by these observations, in this paper, we propose a hierarchical³ graph matching network (HGMM) for computing the graph similarity between any pair of graph-structured objects. HGMM jointly learns graph representations and a graph matching metric function for computing graph similarity in an end-to-end fashion. It consists of a novel node-graph matching network for effectively learning cross-level interaction features between nodes of a graph and a whole graph, and a siamese graph neural network for learning global-level interaction features between two graphs. Our final small prediction networks consume these feature vectors from both cross-level and global-level interactions to perform either graph-graph classification or graph-graph regression tasks, respectively.

Recently proposed work only computes graph similarity by considering either graph-graph classification tasks (with labels $Y = \{-1, 1\}$) [24], or graph-graph regression tasks (with similarity score $Y = [0, 1]$) [1, 2]. To demonstrate the effectiveness of our model, we systematically evaluate the performance of HGMM on four datasets for both the graph-graph classification and regression tasks. Noted that, the graph-graph classification tasks here are different from the general graph classification tasks [44, 26] that only assign each graph with a label. Our graph-graph classification tasks learn a binary label (*i.e.*, similar or dissimilar) for pairs of two graphs instead of one graph. Another important aspect is previous work does not consider the impact of the size of input graphs, which often plays an important role in determining the performance of graph similarity learning. Motivated by this observation, we consider three different ranges of graph sizes to evaluate the robustness of models. In addition, to bridge the gap of the lack of standard datasets for graph similarity learning, we create one new dataset from a real application together with a previously released dataset by [42] for graph-graph classification tasks. Both code and data are available at <https://github.com/kleincup/HGMM>. In brief, we highlight our main contributions as follows:

- We propose a hierarchical graph matching network (HGMM) for computing the graph similarity between any pair of graph-structured objects. HGMM jointly learns graph representations and a graph matching metric function for computing graph similarity in an end-to-end fashion.
- In particular, we propose a novel node-graph matching network for effectively capturing the cross-level interactions between a node embedding of a graph and a corresponding attentive graph-level embedding of another graph.
- Comprehensive experiments demonstrate that HGMM consistently outperforms state-of-the-art graph similarity learning baselines for different tasks (*i.e.*, classification and regression) and also exhibits stronger robustness as the sizes of the two input graphs increase.

2 Problem Formulation

In this section, we briefly introduce the problem formulation. Given a pair of graph inputs (G^1, G^2) , the aim of graph similarity learning in this paper is to produce a similarity score $y = s(G^1, G^2) \in \mathcal{Y}$. The graph $G^1 = (\mathcal{V}^1, \mathcal{E}^1)$ is represented as a set of N nodes $v_i \in \mathcal{V}^1$ with a feature matrix $X^1 \in \mathcal{R}^{N \times d}$, edges $(v_i, v_j) \in \mathcal{E}^1$ (binary or weighted) formulating an adjacency matrix $A^1 \in \mathcal{R}^{N \times N}$, and a degree matrix $D_{ii}^1 = \sum_j A_{ij}^1$. Similarly, the graph $G^2 = (\mathcal{V}^2, \mathcal{E}^2)$ is represented as a set of M nodes $v_i \in \mathcal{V}^2$ with a feature matrix $X^2 \in \mathcal{R}^{M \times d}$, edges $(v_i, v_j) \in \mathcal{E}^2$ (binary or weighted) formulating an adjacency matrix $A^2 \in \mathcal{R}^{M \times M}$, and a degree matrix $D_{ii}^2 = \sum_j A_{ij}^2$. Note that, when performing the graph-graph classification tasks y is the class label $y = \{-1, 1\}$; when performing the graph-graph regression tasks y is the similarity score $y \in [0, 1]$. We train our model based on a set of training triplet of structured input pairs and scalar output score $(G_1^1, G_1^2, y_1), \dots, (G_n^1, G_n^2, y_n) \in \mathcal{G} \times \mathcal{G} \times \mathcal{Y}$.

³The terminology ‘‘hierarchical’’ here means different-level granularity of interactions between a pair of graphs, which is different from the meaning of ‘‘hierarchical pooling’’ operations in [44].

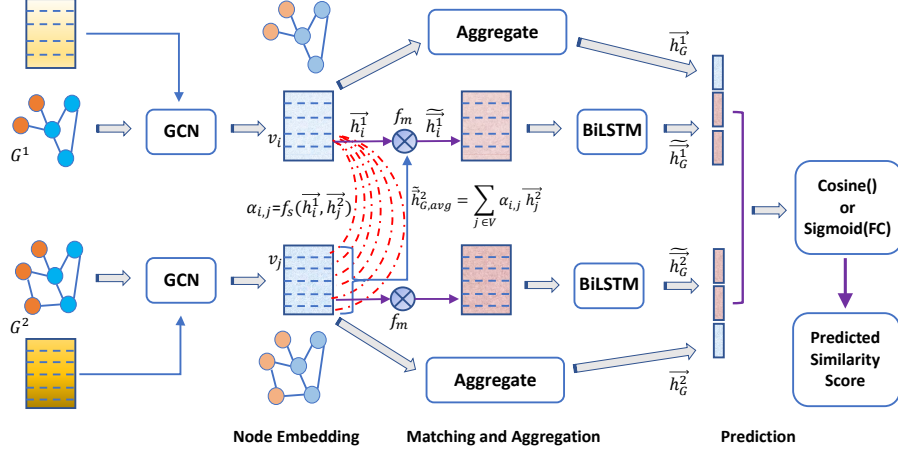


Figure 1: The overview architecture of the full model HGMN, which consists of two components: SGNN and NGMN. At the final prediction layer, we concatenate a total of 6 aggregated graph-level embedding vectors where the middle 4 (pink) are from NGMN and the other 2 (blue) are from SGNN.

3 Hierarchical Graph Matching Networks

In this section, we will introduce two key components of HGMN - Siamese Graph Neural Networks (SGNN) and Node-Graph Matching Networks (NGMN). We first discuss SGNN for learning the global-level interactions between two graphs and then outline NGMN for effectively learning the cross-level node-graph interactions between nodes of one graph and one whole graph. The overall model architecture for HGMN is shown in Figure 1.

3.1 SGNN for Global-level Interaction Learning

The graph-level embeddings contain important information of a graph. Therefore, learning graph-level interactions between two graphs could be an important component for learning the graph similarity of two graphs. To capture the global-level interaction features between two graphs, we employ SGNN, which is based on the Siamese Network architecture [6] that has achieved great success in many applications such as visual recognition [3, 34] and sentence similarity analysis [18, 28]. In general, SGNN consists of 3 components: 1) node embedding layers; 2) graph-level embedding aggregation layers; 3) graph-graph matching and prediction layers.

Node Embedding Layers. We use three-layer graph convolution networks (GCN) with the siamese networks to generate node embeddings $H^l = \{\vec{h}_i^l\}_{i=1}^{\{N,M\}} \in \mathcal{R}^{\{N,M\} \times d^l}$ of both graphs G^1 and G^2 ,

$$H^l = \sigma\left(\bar{A}^l \sigma\left(\bar{A}^l \sigma\left(\bar{A}^l X^l W^{(0)}\right) W^{(1)}\right) W^{(2)}\right), \quad l = \{1, 2\} \quad (1)$$

where σ is the activation function, $\bar{A}^l = (\tilde{D}^l)^{-\frac{1}{2}} \tilde{A}^l (\tilde{D}^l)^{-\frac{1}{2}}$ is the normalized Laplacian matrix for $\tilde{A}^l = A^l + I_{\{N,M\}}$ depending on G^1 or G^2 , and $W^{(i)}, i = \{0, 1, 2\}$ are hidden weighted matrices for each layer. Note that the twin networks share the parameters of GCN when training on the pair of graphs (G^1, G^2) . The number of GCN layers required may depend on the real application graph data.

Graph-level Embedding Aggregation Layers. With the computed node embeddings H^l for each graph, we need to aggregate them to formulate a corresponding graph-level embedding \vec{h}_G^l ,

$$\vec{h}_G^l = \text{Aggregation}\left(\{\vec{h}_i^l\}_{i=1}^{\{N,M\}}\right), \quad l = \{1, 2\}. \quad (2)$$

We employ different aggregation functions such as element-wise max/mean pooling (Max/Avg), element-wise max/mean pooling following a fully connected layer on H^i (FCMax/FCAvg), and an LSTM-based aggregator. Although LSTM is not permutation invariant on a set of node embeddings, it might admit more expressive ability in aggregation and has been applied in previous work [16, 47].

Graph-Graph Matching & Prediction Layers. After the graph-level embeddings \vec{h}_G^1 and \vec{h}_G^2 are computed for G^1 and G^2 , we then use the resulting graph embeddings to compute the graph similarity

score of (G^1, G^2) . As it is common to employ cosine similarity in the classification tasks [42, 14], we directly compute the cosine similarity of two graph-level embeddings,

$$\tilde{y} = s(G^1, G^2) = \text{cosine}(\vec{h}_G^1, \vec{h}_G^2) \quad (3)$$

Differently, the results of the regression tasks are continuous and are set in a range of $[0,1]$. Thus, for the regression tasks, we first concatenate the two graph embeddings into $[\vec{h}_G^1, \vec{h}_G^2]$, employ standard fully connected layers to gradually project the dimension of resulting vector down to 1, and finally perform the sigmoid function to enforce the similarity score in the range of $[0,1]$.

$$\tilde{y} = s(G^1, G^2) = \text{sigmoid}\left(\text{MLP}\left([\vec{h}_G^1, \vec{h}_G^2]\right)\right) \quad (4)$$

For both tasks, we train the SGNN model with the mean square error loss function to compare the computed similarity score \tilde{y} with the ground-truth similarity score y , *i.e.*, $\mathcal{L} = \frac{1}{n} \sum_{i=1}^n (\tilde{y} - y)^2$.

3.2 NGMN for Cross-level Node-Graph Interaction Learning

Although global-level interaction learning could capture the important structural and feature information of two graphs to some extent, it is not enough to capture all important information of two graphs since they ignore other cross-level interactions between parts of two graphs. In particular, existing work has considered either global-level graph-graph interactions or low-level node-node interactions, ignoring the rich cross-level interactions between nodes of a graph and a whole graph. Inspired by these observations, we propose a novel node-graph matching network to effectively learn the cross-level interaction features and illustrate each part in detail as follows.

Node Embedding Layers. Similar as described in Section 3.1, we choose to employ the three-layer GCN to generate node embeddings $H^1 = \{\vec{h}_i^1\}_{i=1}^N \in \mathcal{R}^{N \times d'}$ and $H^2 = \{\vec{h}_j^2\}_{j=1}^M \in \mathcal{R}^{M \times d'}$ for graphs G^1 and G^2 . Conceptually, the node embedding layers of NGMN could be chosen to be an independent GCN or a shared GCN with SGNN. As shown in Figure 1, our NGMN shares the same graph encoder (*i.e.*, GCN) with SGNN due to two reasons: i) it reduces the number of parameters by half, which helps mitigate possible overfitting; ii) it maintains the consistency of the resulting node embeddings for both NGMN and SGNN, potentially leading to more aligned global-level interaction and cross-level interaction features.

Node-Graph Matching Layers. This layer is the key part of NGMN, which can effectively learn the cross-level interactions between nodes of a graph and a whole graph. There are generally two steps for this layer: i) calculate the graph-level embedding of a graph; ii) compare the node embeddings of a graph with the associated graph-level embedding of a whole graph and then produce a similarity feature vector. To build more tight interactions between the two graphs for learning the graph-level embedding of each other, we first calculate the cross-graph attention coefficients between the node $v_i \in \mathcal{V}^1$ in G^1 and all other nodes $v_j \in \mathcal{V}^2$ in G^2 . Similarly, we calculate the cross-graph attention coefficients between the node $v_j \in \mathcal{V}^2$ in G^2 and all other nodes $v_i \in \mathcal{V}^1$ in G^1 . These two cross-graph attention coefficients can be computed with an attention function f_s independently,

$$\alpha_{i,j} = f_s(\vec{h}_i^1, \vec{h}_j^2), v_j \in \mathcal{V}^2 \quad \text{and} \quad \beta_{j,i} = f_s(\vec{h}_j^2, \vec{h}_i^1), v_i \in \mathcal{V}^1 \quad (5)$$

where f_s is the attention function for computing the similarity score. For simplicity, we use cosine function in our experiments but other similarity metrics can be adopted as well. Then, we compute the attentive graph-level embeddings $\tilde{h}_{G,avg}^1$ or $\tilde{h}_{G,avg}^2 \in \mathcal{R}^{d'}$ using the weighted average of the node embeddings of the other graph,

$$\tilde{h}_{G,avg}^2 = \sum_{j \in \mathcal{V}^2} \alpha_{i,j} \vec{h}_j^2 \quad \text{and} \quad \tilde{h}_{G,avg}^1 = \sum_{i \in \mathcal{V}^1} \beta_{j,i} \vec{h}_i^1 \quad (6)$$

Next, we define a multi-perspective matching function f_m to compute the similarity feature vector by comparing two vectors as follows,

$$\tilde{h}(k) = f_m(\vec{x}_1, \vec{x}_2, \vec{w}_k) = f_m(\vec{x}_1 \odot \vec{w}_k, \vec{x}_2 \odot \vec{w}_k), k = 1, \dots, \tilde{d} \quad (7)$$

where $\tilde{h} \in \mathcal{R}^{\tilde{d}}$ is a \tilde{d} -dimension similarity feature vector, $W_m = \{\vec{w}_k\}_{k=1}^{\tilde{d}} \in \mathcal{R}^{d' \times \tilde{d}}$ is a trainable weight matrix and each \vec{w}_i represents a perspective with total \tilde{d} number of perspectives. Notably, f_m

could be any similarity function and we use the cosine similarity metric in our experiments. It is worth noting that the proposed f_m essentially shares a similar spirit with multi-head attention [35], with the difference that multi-head attention uses \tilde{d} number of weighted matrices instead of vectors.

Therefore, we can use f_m to compare the i -th or j -th node embedding of a graph with the corresponding attentive graph-level embedding to capture the cross-level node-graph interactions. The resulting similarity feature vectors \tilde{h}_i^1 or $\tilde{h}_i^2 \in \mathcal{R}^{\tilde{d}}$ (w.r.t node v_i in either G^1 or G^2) can thus be computed by,

$$\tilde{h}_i^1 = f_m(\vec{h}_i^1, \vec{h}_{G,avg}^2, W_m), v_i \in \mathcal{V}^1 \quad \text{and} \quad \tilde{h}_j^2 = f_m(\vec{h}_j^2, \vec{h}_{G,avg}^1, W_m), v_j \in \mathcal{V}^2 \quad (8)$$

After performing node-graph matching over all nodes for both G^1 and G^2 , the newly produced interaction feature matrices $\tilde{H}^1 = \{\tilde{h}_i^1\}_{i=1}^N \in \mathcal{R}^{N \times \tilde{d}}$ and $\tilde{H}^2 = \{\tilde{h}_j^2\}_{j=1}^M \in \mathcal{R}^{M \times \tilde{d}}$ are ready to be fed into the aggregation layers.

Aggregation Layers. To aggregate the cross-level interaction feature matrix from the node-graph matching layer, we employ BiLSTM [19] to aggregate the unordered feature embeddings,

$$\tilde{h}_G^l = \text{BiLSTM}\left(\{\tilde{h}_i^l\}_{i=1}^{\{N,M\}}\right), \quad l = \{1, 2\}. \quad (9)$$

where $\tilde{h}_G^l \in \mathcal{R}^{2\tilde{d}}$ is computed by concatenating the last hidden vectors of two directions and represents the aggregated graph-level embedding for each graph G^1 and G^2 . Although other aggregators can also be used, our extensive experiments show that BiLSTM aggregator achieved consistent better performance over other aggregators (see Appendix A.4). Similar LSTM-type aggregators have also been employed in the previous work [16, 47].

Prediction Layers. After the aggregated graph embeddings \tilde{h}_G^1 and \tilde{h}_G^2 are obtained, we then use these two embeddings to compute the similarity score of $s(G^1, G^2)$. Just like the prediction layer in SGNN, we use Equations (3) and (4) to predict the similarity score for both classification and regression tasks. We also use the same mean square error loss function for the model training.

3.3 Discussions on Our Full Model – HGMN

The full model HGMN combines the advantages of both SGNN and NGMN to capture both global-level graph-graph interaction features and cross-level node-graph interaction features between two graphs. For the final prediction layer of HGMN, we have a total of six aggregated graph embedding vectors where two are \vec{h}_G^1 and \vec{h}_G^2 from SGNN, and another four are \tilde{h}_G^1 and \tilde{h}_G^2 from NGMN.

Complexity. The computation complexity of SGNN is $O((|\mathcal{E}^1| + |\mathcal{E}^2|)dd')$, where the most dominant computation is the sparse matrix-matrix operations in Equation (1). Similarly, the computational complexity of NGMN is $O(NMd + (N + M)d' + (N + M)dd')$, where the most computationally extensive operations are in Equations (6), (7), and (8). Compared to recently proposed work [1, 2, 24], their computational complexities are highly comparable.

4 Experiments

4.1 Datasets, Experimental Setup, and Baselines

Classification Datasets: we evaluate our model on the task of detecting a similarity score (*i.e.*, $Y = \pm 1$) between two binary functions, which is the heart of many binary security problems [12, 42, 11]. As we represent binaries with control flow graphs, detecting the similarity between two binaries can be cast as learning the similarity score $s(G^1, G^2)$ between two control flow graphs G^1 and G^2 . We prepare two datasets generated from two popular open-source softwares: **FFmpeg** and **OpenSSL**. Besides, existing work does not consider the impact of the sizes of graphs on the performance. However, we find the larger the graph size is, the worse the performance is. Therefore, it is important to evaluate the robustness of graph similarity networks in this setting. We thus further split each datasets into 3 sub-datasets ([3, 200], [20,200], and [50,200]) according to the range of graph sizes. ⁴

⁴Although there are many benchmarks for the general graph classification tasks, these cannot be directly used in our graph-graph classification tasks as we cannot simply treat two graphs with the same labels as “similar”.

Table 1: Summary statistics of datasets for both classification & regression tasks.

Tasks	Datasets	Sub-datasets	# of Graphs	# of Functions	AVG # of Nodes	AVG # of Edges	Init Feature Dimensions
classification	FFmpeg	[3, 200]	83,008	10,376	18.83	27.02	6
		[20, 200]	31,696	7,668	51.02	75.88	
		[50, 200]	10,824	3,178	90.93	136.83	
	OpenSSL	[3, 200]	73,953	4,249	15.73	21.97	6
		[20, 200]	15,800	1,073	44.89	67.15	
		[50, 200]	4,308	338	83.68	127.75	
regression	AIDS700	-	700	-	8.90	8.80	29
	LINUX1000	-	1000	-	7.58	6.94	1

Regression Datasets: we evaluate our model on learning the graph edit distance (GED) [46, 13, 30], which measures the structural similarity between two graphs. Formally, GED is defined as the cost of the least expensive sequence of edit operations that transform one graph into another, where an edit operation can be an insertion or a deletion of a node or an edge. In our experiments, we normalize GED as $Y = e^{-[\frac{GED(G^1, G^2)}{(N+M)/2}]} \in [0, 1]$, and evaluate models on two datasets **AIDS700** and **LINUX1000** from [1]. Table 1 shows the statistic for all datasets with more details in Appendix A.1.

Implementation Details. We implement our models using PyTorch 1.1 [29] and train them with Adam optimizer [21]. We use 3 GCN layers with each output dimension of 100 and set the number of perspectives \tilde{d} to 100. For classification tasks, we train the model by running 100 epochs with 0.5e-3 learning rate. At each epoch, we build the pairwise training data as follows. For each graph G in the training subset, we obtain one positive pair $\{(G, G^{pos}), +1\}$ and a corresponding negative pair $\{(G, G^{neg}), -1\}$, where G^{pos} is randomly selected from all control flow graphs that compiled from the same source function as G , and G^{neg} is selected from other graphs. By default, each mini-batch includes 5 positive and 5 negative pairs. For regression tasks, we train the model by 10000 iterations with a mini-batch of 128 graph pairs with 5e-3 learning rate. Each pair is a tuple of $\{(G^1, G^2), s\}$, where s is the ground-truth GED between G^1 and G^2 . Noted that all experiments are conducted on a PC equipped with 8 Intel Xeon 2.2GHz CPU and one NVIDIA GTX 1080 Ti GPU. Other model settings and experiment details can be found in Appendix A.2.1.

Baseline Methods⁵: i) *SimGNN* [1] adopts GCN to encode node features and applies 2 strategies to model the similarity between two graphs: one based on interactions between two graph-level embeddings, another based on histogram features from two sets of node embeddings; ii) *GMN* [24] employs a variant of message passing neural networks and improves the node embeddings of one graph via incorporating the information of attentive neighborhoods of another graph; iii) *GraphSim* [2] extends SimGNN by turning the two sets of node embeddings into a similarity matrix and then processing the matrix with CNNs [23]. Detailed experimental settings are given in Appendix A.2.2.

Note that we have two variants of the full model HGMM: **HGMM (FCMax)** and **HGMM (BiLSTM)**, where SGNN uses either the FCMax or BiLSTM aggregator, respectively. We repeat all experiments 5 times and report the mean and standard deviation of results, with the best performance in **bold**.

4.2 Comparison with Baseline Methods

Comparison on the Graph-Graph Classification Tasks. For graph-graph classification tasks, we measure the *Area Under the ROC Curve (AUC)* [5] of different models. As shown in Table 2, our models (both full model HGMM or key component NGMM) clearly achieve state-of-the-art performance on all 6 sub-datasets for both **FFmpeg** and **OpenSSL**. Particularly when the graph size increases, both HGMM and NGMM models show better and more robust performance than state-of-the-art methods. In addition, compared with SGNN (Max), NGMM shows superior performance by a large margin, demonstrating the benefits of the multi-perspective node-graph matching mechanism that captures the cross-level interaction features between node embeddings of a graph and the graph-level embedding of another graph. HGMM (*i.e.*, NGMM+SGNN) further improves the performance of NGMM together with global-level interaction features learned from SGNN (see more experiments of SGNN with other aggregation functions in Appendix A.3).

⁵As the three baseline methods only consider classification tasks or regression tasks, we slightly adjust the last layer of model or loss function of each baseline in order to make fair comparisons on both tasks.

Table 2: Summary of classification results in terms of AUC scores (%).

Model	FFmpeg			OpenSSL		
	[3, 200]	[20, 200]	[50, 200]	[3, 200]	[20, 200]	[50, 200]
SimGNN	95.38±0.76	94.31±1.01	93.45±0.54	95.96±0.31	93.58±0.82	94.25±0.85
GMN	94.15±0.62	95.92±1.38	94.76±0.45	96.43±0.61	93.03±3.81	93.91±1.65
GraphSim	97.46±0.30	96.49±0.28	94.48±0.73	96.84±0.54	94.97±0.98	93.66±1.84
SGNN	93.92±0.07	93.82±0.28	85.15±1.39	91.07±0.10	88.94±0.47	82.10±0.51
NGMN	97.73±0.11	98.29±0.21	96.81±0.96	96.56±0.12	97.60±0.29	92.89±1.31
HGMN (FCMax)	98.07±0.06	98.29±0.10	97.83±0.11	96.87±0.24	97.59±0.24	95.58±1.13
HGMN (BiLSTM)	97.56±0.38	98.12±0.04	97.16±0.53	96.90±0.10	97.31±1.07	95.87±0.88

Comparison on the Graph-Graph Regression Tasks. For the regression tasks of computing the normalized GED between two graphs, we evaluate the models using Mean Square Error (mse), Spearman’s Rank Correlation Coefficient (ρ) [33], Kendall’s Rank Correlation Coefficient (τ) [20], and precision at k ($p@k$). All results of both **AIDS700** and **LINUX1000** datasets are summarized in Table 3. Although GraphSim shows better performance than the other two baselines, our models (the full model HGMN and key component NGMN) outperform all baselines on both datasets in terms of most evaluation metrics. Moreover, compared with SGNN (Max), NGMN achieves much better performance (see more in Appendix A.3). It highlights the importance of our proposed node-graph matching mechanism, which could effectively capture cross-level node-graph interactions between nodes of a graph and a whole graph in NGMN. HGMN (*i.e.*, SGNN+NGMN) further improves the performance of NGMN together with global-level interaction features learned from SGNN.

Table 3: Summary of regression results on **AIDS700** and **LINUX1000**.

Datasets	Model	$mse (10^{-3})$	ρ	τ	p@10	p@20
AIDS700	SimGNN	1.376±0.066	0.824±0.009	0.665±0.011	0.400±0.023	0.489±0.024
	GMN	4.610±0.365	0.672±0.036	0.497±0.032	0.200±0.018	0.263±0.018
	GraphSim	1.919±0.060	0.849±0.008	0.693±0.010	0.446±0.027	0.525±0.021
	SGNN	2.822±0.149	0.765±0.005	0.588±0.004	0.289±0.016	0.373±0.012
	NGMN	1.191±0.048	0.904±0.003	0.749±0.005	0.465±0.011	0.538±0.007
	HGMN (FCMax)	1.205±0.039	0.904±0.002	0.749±0.003	0.457±0.014	0.532±0.016
	HGMN (BiLSTM)	1.169±0.036	0.905±0.002	0.751±0.003	0.456±0.019	0.539±0.018
LINUX 1000	SimGNN	2.479±1.038	0.912±0.031	0.791±0.046	0.635±0.328	0.650±0.283
	GMN	2.571±0.519	0.906±0.023	0.763±0.035	0.888±0.036	0.856±0.040
	GraphSim	0.471±0.043	0.976±0.001	0.931±0.003	0.956±0.006	0.942±0.007
	SGNN	11.832±0.698	0.566±0.022	0.404±0.017	0.226±0.106	0.492±0.190
	NGMN	1.561±0.020	0.945±0.002	0.814±0.003	0.743±0.085	0.741±0.086
	HGMN (FCMax)	1.575±0.627	0.946±0.019	0.817±0.034	0.807±0.117	0.784±0.108
	HGMN (BiLSTM)	0.439±0.143	0.985±0.005	0.919±0.016	0.955±0.011	0.943±0.014

4.3 Ablation Studies

Different Attention Functions. As discussed in Section 3.2, the proposed multi-perspective matching function shares similar spirits with the multi-head attention mechanism [35], which makes it interesting to compare them. Therefore, we investigate the impact of these two different attention mechanisms for the proposed NGMN model with classification results showed in Table 4. Interestingly, our proposed multi-perspective attention mechanism consistently outperforms the results of the multi-head attention mechanism by quite a large margin. We suspect that our proposed multi-perspective attention uses vectors attention weights which may significantly reduce the potential overfitting.

Table 4: Classification results of multi-perspectives versus multi-heads in terms of AUC scores(%).

Model	FFmpeg			OpenSSL		
	[3, 200]	[20, 200]	[50, 200]	[3, 200]	[20, 200]	[50, 200]
Multi-Perspectives ($\tilde{d} = 100$)	97.73±0.11	98.29±0.21	96.81±0.96	96.56±0.12	97.60±0.29	92.89±1.31
Multi-Heads ($K = 6$)	91.18±5.91	77.49±5.21	68.15±6.97	92.81±5.21	85.43±5.76	56.87±7.53

Different Numbers of Perspectives. We further investigate the impact of different number of perspectives adopted by the node-graph matching layer of the NGMN model for classification tasks. Following the same settings of previous experiments, we only change the number of perspectives (*i.e.*, $\tilde{d} = 50/75/100/125/150$) of NGMN. From Table 5, it is clearly seen that the AUC score of NGMN

does not increase as the number of perspectives grows. We thus conclude that our model performance is not sensitive to the number of perspective \tilde{d} (from 50 to 150) and we make $\tilde{d} = 100$ by default.

Table 5: Classification results of different number of perspectives in terms of AUC scores(%).

Model	FFmpeg			OpenSSL		
	[3, 200]	[20, 200]	[50, 200]	[3, 200]	[20, 200]	[50, 200]
NGMN ($\tilde{d} = 50$)	98.11±0.14	97.76±0.14	96.93±0.52	97.38±0.11	97.03±0.84	93.38±3.03
NGMN ($\tilde{d} = 75$)	97.99±0.09	97.94±0.14	97.41±0.05	97.09±0.25	98.66±0.11	92.10±4.37
NGMN ($\tilde{d} = 100$)	97.73±0.11	98.29±0.21	96.81±0.96	96.56±0.12	97.60±0.29	92.89±1.31
NGMN ($\tilde{d} = 125$)	98.10±0.03	98.06±0.08	97.26±0.36	96.73±0.33	98.67±0.11	96.03±2.08
NGMN ($\tilde{d} = 150$)	98.32±0.05	98.11±0.07	97.92±0.09	96.50±0.31	98.04±0.03	97.13±0.36

Different GNNs. We investigate the impact of different GNNs including GraphSAGE [16], GIN [41], and GGNN [25] adopted by the node embedding layer of our NGMN models for both classification and regression tasks. Table 6 presents the results of classification tasks (see the regression results from Table 12 in Appendix A.5). In general, the performance of different GNNs is quite similar for all datasets of both classification and regression tasks, which indicates that our model is not sensitive to the choice of GNNs in the node embedding layers. An interesting observation is that NGMN-GGNN performs even better than our default NGMN-GCN on both **FFmpeg** and **OpenSSL** datasets. This shows that our model can be further improved by adopting more advanced GNN models or choosing the most appropriate GNNs according to different application tasks.

Table 6: Classification results of different GNNs in terms of AUC scores (%).

Model	FFmpeg			OpenSSL		
	[3, 200]	[20, 200]	[50, 200]	[3, 200]	[20, 200]	[50, 200]
NGMN-GCN (Our)	97.73±0.11	98.29±0.21	96.81±0.96	96.56±0.12	97.60±0.29	92.89±1.31
NGMN-GraphSAGE	97.31±0.56	98.21±0.13	97.88±0.15	96.13±0.30	97.30±0.72	93.66±3.87
NGMN-GIN	97.97±0.08	98.06±0.22	94.66±4.01	96.98±0.20	97.42±0.48	92.29±2.23
NGMN-GGNN	98.42±0.41	99.77±0.07	97.93±1.18	99.35±0.06	98.51±1.04	94.17±7.74

5 Related Work

Conventional Graph Matching. In general, graph matching can be categorized into *exact graph matching* and *error-tolerant graph matching*. Exact graph matching aims to find a strict correspondence between two (in large parts) identical graphs being matched, while error-tolerant graph matching allows matching between completely non-identical graphs [30]. In real-world applications, the constraint of exact graph matching is too rigid, and thus an amount of work has been proposed to solve the error-tolerant graph matching problem, which is usually quantified by a specific similarity metric, such as GED, maximum common subgraph (MCS) [8], or even more coarse binary similarity, according to different application backgrounds. For GED and MCS, both of them are well-studied NP-hard problems and suffer from exponential computational complexity and huge memory requirements for exact solutions in practice [8, 27, 46, 4].

Graph Similarity Computation and Graph Matching Networks. Considering the great significance and challenge of computing the graph similarity, various approximation methods have been proposed for improvements for better accuracy and efficiency, including traditional heuristic methods [13, 46, 30, 40, 45, 39] and recent data-driven graph matching networks [1, 2, 24], as detailed in the baselines of Section 4.1. Our research belongs to the graph matching networks, but differs from prior work in two main aspects. First, unlike prior work only consider graph-level or node-level interaction features, our HGMN model successfully captures richer interactions between nodes of a graph and a whole graph. Second, our work is the first one to systematically evaluate the performance on both graph-graph classification and regression tasks as well as the size of input graphs.

6 Conclusion and Future Work

In this paper, we presented a novel hierarchical graph matching network (HGMN) for computing the graph similarity between any pair of graph-structured objects. Our model jointly learned graph embeddings and a data-driven graph matching metric for computing graph similarity in an end-to-end

fashion. We further proposed a new node-graph matching network for effectively learning cross-level interactions between two graphs beyond low-level node-node and global-level graph-graph interactions. Our extensive experimental results correlated the superior performance compared with state-of-the-art baselines on both graph-graph classification and regression tasks. One interesting future direction is to adapt our HGMM model for solving different real-world applications such as unknown malware detection, text matching and entailment, and knowledge graph question answering.

References

- [1] Y. Bai, H. Ding, S. Bian, T. Chen, Y. Sun, and W. Wang. Simgnn: A neural network approach to fast graph similarity computation. In *Proceedings of the Twelfth ACM International Conference on Web Search and Data Mining*, pages 384–392. ACM, 2019.
- [2] Y. Bai, H. Ding, K. Gu, Y. Sun, and W. Wang. Learning-based efficient graph similarity computation via multi-scale convolutional set matching. In *Thirty-Forth AAAI Conference on Artificial Intelligence*, 2020.
- [3] L. Bertinetto, J. Valmadre, J. F. Henriques, A. Vedaldi, and P. H. Torr. Fully-convolutional siamese networks for object tracking. In *European conference on computer vision*, pages 850–865. Springer, 2016.
- [4] D. B. Blumenthal and J. Gamper. On the exact computation of the graph edit distance. *Pattern Recognition Letters*, 2018.
- [5] A. P. Bradley. The use of the area under the roc curve in the evaluation of machine learning algorithms. *Pattern Recognition*, 1997.
- [6] J. Bromley, I. Guyon, Y. LeCun, E. Säckinger, and R. Shah. Signature verification using a "siamese" time delay neural network. In *Advances in neural information processing systems*, pages 737–744, 1994.
- [7] M. M. Bronstein, J. Bruna, Y. LeCun, A. Szlam, and P. Vandergheynst. Geometric deep learning: going beyond euclidean data. *IEEE Signal Processing Magazine*, 34(4):18–42, 2017.
- [8] H. Bunke. On a relation between graph edit distance and maximum common subgraph. *Pattern Recognition Letters*, 18(8):689–694, 1997.
- [9] H. Bunke and G. Allermann. Inexact graph matching for structural pattern recognition. *Pattern Recognition Letters*, 1(4):245–253, 1983.
- [10] T. S. Caetano, J. J. McAuley, L. Cheng, Q. V. Le, and A. J. Smola. Learning graph matching. *IEEE transactions on pattern analysis and machine intelligence*, 31(6):1048–1058, 2009.
- [11] S. H. Ding, B. C. Fung, and P. Charland. Asm2vec: Boosting static representation robustness for binary clone search against code obfuscation and compiler optimization. In *IEEE Symposium on Security and Privacy (S&P)*, 2019.
- [12] Q. Feng, R. Zhou, C. Xu, Y. Cheng, B. Testa, and H. Yin. Scalable graph-based bug search for firmware images. In *Proceedings of the 2016 ACM SIGSAC Conference on Computer and Communications Security*, 2016.
- [13] X. Gao, B. Xiao, D. Tao, and X. Li. A survey of graph edit distance. *Pattern Analysis and applications*, 13(1):113–129, 2010.
- [14] X. Gu, H. Zhang, and S. Kim. Deep code search. In *2018 IEEE/ACM 40th International Conference on Software Engineering (ICSE)*, pages 933–944. IEEE, 2018.
- [15] M. Guo, E. Chou, D.-A. Huang, S. Song, S. Yeung, and L. Fei-Fei. Neural graph matching networks for fewshot 3d action recognition. In *Proceedings of the European Conference on Computer Vision (ECCV)*, pages 653–669, 2018.
- [16] W. Hamilton, Z. Ying, and J. Leskovec. Inductive representation learning on large graphs. In *Advances in Neural Information Processing Systems*, 2017.
- [17] P. E. Hart, N. J. Nilsson, and B. Raphael. A formal basis for the heuristic determination of minimum cost paths. *IEEE transactions on Systems Science and Cybernetics*, 4(2):100–107, 1968.
- [18] H. He, K. Gimpel, and J. Lin. Multi-perspective sentence similarity modeling with convolutional neural networks. In *Proceedings of the 2015 Conference on Empirical Methods in Natural Language Processing*, pages 1576–1586, 2015.

- [19] S. Hochreiter and J. Schmidhuber. Long short-term memory. *Neural computation*, 1997.
- [20] M. G. Kendall. A new measure of rank correlation. *Biometrika*, 1938.
- [21] D. P. Kingma and J. Ba. Adam: A method for stochastic optimization. In *International Conference on Learning Representations*, 2015.
- [22] T. N. Kipf and M. Welling. Semi-supervised classification with graph convolutional networks. In *International Conference on Learning Representations*, 2017.
- [23] A. Krizhevsky, I. Sutskever, and G. E. Hinton. Imagenet classification with deep convolutional neural networks. In *Advances in neural information processing systems*, pages 1097–1105, 2012.
- [24] Y. Li, C. Gu, T. Dullien, O. Vinyals, and P. Kohli. Graph matching networks for learning the similarity of graph structured objects. *ICML*, 2019.
- [25] Y. Li, D. Tarlow, M. Brockschmidt, and R. Zemel. Gated graph sequence neural networks. *International Conference on Learning Representations*, 2016.
- [26] Y. Ma, S. Wang, C. C. Aggarwal, and J. Tang. Graph convolutional networks with eigenpooling. In *Proceedings of the 25th ACM SIGKDD International Conference on Knowledge Discovery & Data Mining*, pages 723–731, 2019.
- [27] J. J. McGregor. Backtrack search algorithms and the maximal common subgraph problem. *Software: Practice and Experience*, 12(1):23–34, 1982.
- [28] J. Mueller and A. Thyagarajan. Siamese recurrent architectures for learning sentence similarity. In *Thirtieth AAAI Conference on Artificial Intelligence*, 2016.
- [29] A. Paszke, S. Gross, S. Chintala, G. Chanan, E. Yang, Z. DeVito, Z. Lin, A. Desmaison, L. Antiga, and A. Lerer. Automatic differentiation in pytorch, 2017.
- [30] K. Riesen. Structural pattern recognition with graph edit distance. In *Advances in computer vision and pattern recognition*. Springer, 2015.
- [31] K. Riesen, S. Emmenegger, and H. Bunke. A novel software toolkit for graph edit distance computation. In *International Workshop on Graph-Based Representations in Pattern Recognition*, pages 142–151. Springer, 2013.
- [32] K. Riesen, X. Jiang, and H. Bunke. Exact and inexact graph matching: Methodology and applications. In *Managing and Mining Graph Data*, pages 217–247. Springer, 2010.
- [33] C. Spearman. The proof and measurement of association between two things. *American Journal of Psychology*, 1904.
- [34] R. R. Variator, M. Haloi, and G. Wang. Gated siamese convolutional neural network architecture for human re-identification. In *European conference on computer vision*, pages 791–808. Springer, 2016.
- [35] A. Vaswani, N. Shazeer, N. Parmar, J. Uszkoreit, L. Jones, A. N. Gomez, Ł. Kaiser, and I. Polosukhin. Attention is all you need. In *Advances in neural information processing systems*, pages 5998–6008, 2017.
- [36] P. Velickovic, G. Cucurull, A. Casanova, A. Romero, P. Liò, and Y. Bengio. Graph attention networks. In *International Conference on Learning Representations*, 2018.
- [37] S. Wang, Z. Chen, X. Yu, D. Li, J. Ni, L.-A. Tang, J. Gui, Z. Li, H. Chen, and P. S. Yu. Heterogeneous graph matching networks for unknown malware detection. In *Proceedings of International Joint Conference on Artificial Intelligence*, 2019.
- [38] X. Wang, X. Ding, A. K. Tung, S. Ying, and H. Jin. An efficient graph indexing method. In *2012 IEEE 28th International Conference on Data Engineering*, 2012.

- [39] L. Wu, I. E.-H. Yen, F. Xu, P. Ravikumar, and M. Witbrock. D2ke: From distance to kernel and embedding. *arXiv preprint arXiv:1802.04956*, 2018.
- [40] L. Wu, I. E.-H. Yen, Z. Zhang, K. Xu, L. Zhao, X. Peng, Y. Xia, and C. Aggarwal. Scalable global alignment graph kernel using random features: From node embedding to graph embedding. In *Proceedings of the 25th ACM SIGKDD International Conference on Knowledge Discovery & Data Mining*, pages 1418–1428, 2019.
- [41] K. Xu, W. Hu, J. Leskovec, and S. Jegelka. How powerful are graph neural networks? In *International Conference on Learning Representations*, 2019.
- [42] X. Xu, C. Liu, Q. Feng, H. Yin, L. Song, and D. Song. Neural network-based graph embedding for cross-platform binary code similarity detection. In *Proceedings of the 2017 ACM SIGSAC Conference on Computer and Communications Security*, 2017.
- [43] X. Yan and J. Han. gspan: Graph-based substructure pattern mining. In *Proceedings of IEEE International Conference on Data Mining*, pages 721–724. IEEE, 2002.
- [44] Z. Ying, J. You, C. Morris, X. Ren, W. Hamilton, and J. Leskovec. Hierarchical graph representation learning with differentiable pooling. In *Advances in Neural Information Processing Systems*, pages 4800–4810, 2018.
- [45] T. Yoshida, I. Takeuchi, and M. Karasuyama. Learning interpretable metric between graphs: Convex formulation and computation with graph mining. In *Proceedings of the 25th ACM SIGKDD International Conference on Knowledge Discovery & Data Mining*, pages 1026–1036. ACM, 2019.
- [46] Z. Zeng, A. K. Tung, J. Wang, J. Feng, and L. Zhou. Comparing stars: On approximating graph edit distance. *Proceedings of the VLDB Endowment*, 2(1):25–36, 2009.
- [47] C. Zhang, D. Song, C. Huang, A. Swami, and N. V. Chawla. Heterogeneous graph neural network. In *Proceedings of the 25th ACM SIGKDD International Conference on Knowledge Discovery & Data Mining*, 2019.

A Appendix

A.1 Datasets

A.1.1 Classification Datasets

In our evaluation, two binary functions that are compiled from the same source code but under different settings (architectures, compilers, optimization levels, etc) are considered to be semantically similar to each other. It is noted that one source code function, after compiled with different settings (architectures, compilers, optimization levels, etc), can generate various binary functions. To learn the similarity scores from pairs of binary functions, we represent those binary functions with control flow graphs, whose nodes represent the basic blocks (a basic block is a sequence of instructions without jumps) and edges represent control flow paths between these basic blocks. Thus, detecting the similarity between two binary functions can be cast as the problem of learning the similarity score $s(G^1, G^2)$ between two control flow graphs G^1 and G^2 , where $s(G^1, G^2) = +1$ indicates G^1 and G^2 are similar; otherwise $s(G^1, G^2) = -1$ indicates dissimilar. We prepare two benchmark datasets generated from two popular open-source softwares: **FFmpeg** and **OpenSSL**, to evaluate our model on the graph-graph classification tasks.

For **FFmpeg**, we prepare the corresponding control flow graph (CFG) dataset as the benchmark dataset to detect binary function similarity. First, we compile *FFmpeg 4.1.4* using 2 different compilers *gcc 5.4.0* and *clang 3.8.0*, and 4 different compiler optimization levels (*O0-O3*), and generate 8 different binary files. Second, these 8 generated binaries are disassembled using IDA Pro,⁶ which can produce CFGs for all disassembled functions. Finally, for each basic block in CFGs, we extract 6 block-level numeric features as the initial node representation based on IDAPython (a python-based plugin in IDA Pro).

OpenSSL is built from OpenSSL (v1.0.1f and v1.0.1u) using *gcc 5.4* in three different architectures (x86, MIPS, and ARM), and four different optimization levels (*O0-O3*). The **OpenSSL** dataset that we evaluate is previously released by [42] and publicly available⁷ with prepared 6 block-level numeric features.

Overall, for both **FFmpeg** and **OpenSSL** datasets, each node in the CFGs are initialized with 6 block-level numeric features: # of string constants, # of numeric constants, # of total instructions, # of transfer instructions, # of call instructions, and # of arithmetic instructions.

A.1.2 Regression Datasets

Instead of directly computing the graph edit distance (GED) between two graphs G^1 and G^2 , we try to learn a similarity score $s(G^1, G^2)$, which is the normalized exponential of GED in the range of (0, 1]. To be specific, $s(G^1, G^2) = \exp^{-normGED(G^1, G^2)}$, $normGED(G^1, G^2) = \frac{GED(G^1, G^2)}{(|G^1| + |G^2|)/2}$, where $|G^1|$ or $|G^2|$ denotes the number of nodes of G^1 or G^2 , and $normGED(G^1, G^2)$ or $GED(G^1, G^2)$ denotes the normalized/un-normalized GED between G^1 and G^2 .

We employ both **AIDS700** and **LINUX1000** released by [1], which are publicly available.⁸ Each dataset contains a set of graph pairs as well as their ground-truth GED scores, which are computed by exponential-time exact GED computation algorithm A^* [17, 31]. As the ground-truth GEDs of another dataset **IMDB-MULTI** are provided with in-exact approximations, we thus do not consider this dataset in our experiments.

AIDS700 is a subset of the *AIDS* dataset, a collection of AIDS antiviral screen chemical compounds from the Development Therapeutics Program (DTP) in the National Cancer Institute (NCI).⁹ Originally, *AIDS* contains 42687 chemical compounds, where each of them can be represented as a graph with atoms as nodes and bonds as edges. To avoid calculating the ground-truth GED between two graphs with a large number of nodes, the authors of [1] create the **AIDS700** dataset that contains 700 graphs with 10 or fewer nodes. For each graph in **AIDS700**, every node is labeled with the element type of its atom and every edge is unlabeled (*i.e.*, bonds features are ignored).

⁶IDA Pro disassembler, <https://www.hex-rays.com/products/ida/index.shtml>.

⁷<https://github.com/xiaojunxu/dnn-binary-code-similarity>.

⁸<https://github.com/yunshengb/SimGNN>.

⁹<https://wiki.nci.nih.gov/display/NCIDTPdata/AIDS+Antiviral+Screen+Data>

LINUX1000 is also a subset dataset of Linux that introduced in [38]. The original Linux dataset is a collection of 48747 program dependence graphs generated from Linux kernel. In this case, each graph is a static representation of data flow and control dependency within one function, with each node assigned to one statement and each edge describing the dependency between two statements. For the same reason as above that avoiding calculating the ground-truth GED between two graphs with a large number of nodes, the **LINUX1000** dataset used in [1] is randomly selected and contains 1000 graphs with 10 or fewer nodes. For each graph in **LINUX1000**, both nodes and edges are unlabeled.

For both classification and regression datasets, Table 7 provides more detailed statistics. In our evaluation, for the classification tasks, we split each dataset into three disjoint subsets of *binary functions* for training/validation/testing. In the regression tasks, we first split graphs of each dataset into training, validation, and testing sets, and then build the pairwise training/validation/testing data as the previous work [1].

Table 7: Summary statistics of datasets for both classification & regression tasks.

Tasks	Datasets	Sub-datasets	# of Graphs	# of Functions	# of Nodes (Min/Max/AVG)	# of Edges (Min/Max/AVG)	# of Degrees (Min/Max/AVG)
classification	FFmpeg	[3, 200]	83,008	10,376	(3/200/18.83)	(2/332/27.02)	(1.25/4.33/2.59)
		[20, 200]	31,696	7,668	(20/200/51.02)	(20/352/75.88)	(1.90/4.33/2.94)
		[50, 200]	10,824	3,178	(50/200/90.93)	(52/352/136.83)	(2.00/4.33/3.00)
	OpenSSL	[3, 200]	73,953	4,249	(3/200/15.73)	(1/376/21.97)	(0.12/3.95/2.44)
		[20, 200]	15,800	1,073	(20/200/44.89)	(2/376/67.15)	(0.12/3.95/2.95)
		[50, 200]	4,308	338	(50/200/83.68)	(52/376/127.75)	(2.00/3.95/3.04)
regression	AIDS700	-	700	-	(2/10/8.90)	(1/14/8.80)	(1.00/2.80/1.96)
	LINUX1000	-	1000	-	(4/10/7.58)	(3/13/6.94)	(1.50/2.60/1.81)

A.2 More Experimental Setup

A.2.1 Other experimental settings for our models

For SGNN, we use three GCN layers in the node embedding layer and each of the GCNs has an output dimension of 100. We use ReLU as the activation function along with a dropout layer after each GCN layer with dropout rate being 0.1. In the graph-level embedding aggregation layer of SGNN, we can employ different aggregation functions (i.e., Max, FCMax, Avg, FCAvg and BiLSTM) as stated previously in Section 3.1. For NGMN, We set the number of perspectives \tilde{d} to 100. We also employed different aggregation functions similar to SGNN and found that BiLSTM consistently performs better than others (see Appendix A.4). Thus, for NGMN, we take BiLSTM as the default aggregation function and we make its hidden size equal to the dimension of node embeddings. For each graph, we concatenate the last hidden vector of two directions of BiLSTM, which results in a 200-dimension vector as the graph embedding.

A.2.2 Detailed experimental settings for baseline models

In principle, we follow the same experimental settings as the baseline methods of their original papers and adjust a few settings to fit specific tasks. For instance, **SimGNN** is originally used for graph-graph regression tasks, we modify the final layer of model architecture so that it can be used to evaluate graph-graph classification tasks fairly. Thus, detailed experimental settings of all three baseline methods for both classification and regression tasks are given as follows.

SimGNN: SimGNN firstly adopts three-layer GCN to encode each node of a pair of graphs into a vector. Then, SimGNN employs a two-stage strategy to model the similarity between the two graphs: i) it uses Neural Tensor Network (NTN) module to interact two graph-level embeddings that aggregated by a node attention mechanism; ii) it uses the histogram features extracted from the pairwise node-node similarity scores. Finally, the features learned from the two-stage strategy are concatenated to feed into multiple fully connected layers to obtain a final prediction.

For the graph-graph regression tasks, the output dimensions for the three-layer GCNs are 64, 32, and 16, respectively. The number of K in NTN and the number of histogram bins are both set to 16. Four fully connected layers are employed to reduce the dimension of concatenated results from 32 to 16, 16 to 8, 8 to 4, 4 to 1. As for training, the mean square error (MSE) loss function is used to train the

model with Adam optimizer. The learning rate is set to 0.001 and the batch size is set to 128. We set the number of iterations to 10,000 and select the best model based on the lowest validation loss.

To fairly compare our model with SimGNN in evaluating graph-graph classification tasks, we adjust the settings of SimGNN as follows. We follow the same architecture of SimGNN in regression tasks except that the output dimension of the last connected layer is set to 2. We apply a softmax operation over the output of SimGNN to get the predicted binary label for the graph-graph classification tasks. As for training, we use the cross-entropy loss function to train our model and set the number of epochs to 100. Other training hyper-parameters are kept the same as the regression tasks.

GMN: The spirit of GMN is improving the node embeddings of one graph by incorporating the implicit neighbors of another graph through a soft attention mechanism. GMN follows a similar model architecture of the neural message passing network with three components: encoder layer that maps the node and edge to initial vector features of node and edge, propagation layer further update the node embeddings through proposed strategies and an aggregator that compute a graph-level representation for each graph.

For the graph-graph classification tasks, we use 1-layer MLP as the node/edge encoder and set the number of rounds of propagation to 5. The dimension of the node feature is set to 32, and the dimension of graph-level representation is set to 128. The Hamming distance is employed to compute the distance of two graph-level representation vectors. Based on the Hamming distance, we train the model with the margin-based pairwise loss function for 100 epochs in which validation is carried out per epoch. Adam optimizer is used with learning rate of 0.001 and batch size 10.

In order to enable fair comparisons with GMN for graph-graph regression tasks, we adjust the GMN architecture by concatenating the graph-level representation of two graphs and feeding it into a four-layer fully connected layers like SimGNN so that the final output dimension is reduced to 1. As for training, we use mean square loss function with batch size 128. Other settings remain the same as the classification tasks.

GraphSim: The main idea of GraphSim is to convert the graph similarity computation problems into pattern recognition problems. GraphSim first employs GCN to generate node embeddings of the pair of graphs, then turns the two sets of node embedding into a similarity matrix consisting of the pairwise node-node interaction similarity scores, feeds these matrices into convolutional neural networks (CNN), and finally concatenates the results of CNN to multiple fully connected layers to obtain a final predicted graph-graph similarity score.

For the graph-graph regression tasks, three layers of GCN are employed with each output dimension being set to 128, 64, and 32, respectively. The following architecture of CNNs is used: $Conv(6, 1, 1, 16)$, $maxpool(2)$, $Conv(6, 1, 16, 32)$, $maxpool(2)$, $Conv(5, 1, 32, 64)$, $maxpool(2)$, $Conv(5, 1, 64, 128)$, $maxpool(3)$, $Conv(5, 1, 128, 128)$, $maxpool(3)$. Numbers in $Conv()$ and $maxpool()$ indicates $Conv(window\ size, kernel\ stride, input\ channels, output\ channels)$ and $maxpool(pooling\ size)$. Eight fully connected layers are used to reduce the dimension of the concatenated results from CNNs, from 384 to 256, 256 to 128, 128 to 64, 64 to 32, 32 to 16, 16 to 8, 8 to 4, 4 to 1. As for training, the mean square error (MSE) loss function is used to train the model with Adam optimizer. The learning rate is set to 0.001 and the batch size is set to 128. Similar to SimGNN, we set the number of iterations to 10,000 and select the best model based on the lowest validation loss.

To make a fair comparison of our model with GraphSim in our evaluation, we also adjust GraphSim to solve the graph-graph classification tasks. We follow the same architecture of GraphSim in regression tasks except that seven connected layers are used instead of eight. The output dimension of final connected layers is set to 2, and we apply a softmax operation over it to get the predicted binary label for the classification tasks. As for training, we use the cross-entropy loss function to train our model and set the number of epochs to 100. Other training hyper-parameters are kept the same as the regression tasks.

A.2.3 Detailed experimental setup for different GNNs

When performing experiments to see how different GNNs affect the performance of NGMN, we only replace GCN with GraphSAGE, GIN, and GGNN using the geometric deep learning library -

PyTorch Geometric¹⁰. More specifically, for GraphSAGE, we used a 3-layer GraphSAGE GNN with their output dimensions all set to 100. For GIN, we used 3 GIN modules with a 1-layer MLP with output dimension 100 as the learnable function. For GGNN, we used 3 one-layer propagation models to replace the 3 GCNs in our original setting and also set their output dimensions to 100.

A.3 SGNN with different aggregation functions for both classification & regression tasks

To further compare our models with the SGNN models, we train and evaluate several SGNN models with different aggregation functions, such as Max, FCMax, Avg, FCAvg, and BiLSTM. The classification results and regression results are summarized in Table 8 and Table 9, respectively. For both classification and regression tasks, our models (the full model HGMN and key component NGMN) show statistically significant improvement over all SGNN models with different aggregation functions, which indicates the advantage of the proposed node-graph matching network.

Table 8: Classification results of SGNN models with different aggregation functions VS. NGMN and HGMN in term of AUC scores (%).

Model	FFmpeg			OpenSSL		
	[3, 200]	[20, 200]	[50, 200]	[3, 200]	[20, 200]	[50, 200]
SGNN (BiLSTM)	96.92±0.13	97.62±0.13	96.35±0.33	95.24±0.06	96.30±0.27	93.99±0.62
SGNN (Max)	93.92±0.07	93.82±0.28	85.15±1.39	91.07±0.10	88.94±0.47	82.10±0.51
SGNN (FCMax)	95.37±0.04	96.29±0.14	95.98±0.32	92.64±0.15	93.79±0.17	93.21±0.82
SGNN (Avg)	95.61±0.05	96.09±0.05	96.70±0.13	92.89±0.09	93.90±0.24	94.12±0.35
SGNN (FCAvg)	95.18±0.03	95.74±0.15	96.43±0.16	92.70±0.09	93.72±0.19	93.49±0.30
NGMN	97.73±0.11	98.29±0.21	96.81±0.96	96.56±0.12	97.60±0.29	92.89±1.31
HGMN (Max)	97.44±0.32	97.84±0.40	97.22±0.36	94.77±1.80	97.44±0.26	94.06±1.60
HGMN (FCMax)	98.07±0.06	98.29±0.10	97.83±0.11	96.87±0.24	97.59±0.24	95.58±1.13
HGMN (BiLSTM)	97.56±0.38	98.12±0.04	97.16±0.53	96.90±0.10	97.31±1.07	95.87±0.88

Table 9: Regression results of SGNN models with different aggregation functions VS. NGMN and HGMN on **AIDS700** and **LINUX1000**.

Datasets	Model	$mse (10^{-3})$	ρ	τ	p@10	p@20
AIDS700	SGNN (BiLSTM)	1.422±0.044	0.881±0.005	0.718±0.006	0.376±0.020	0.472±0.014
	SGNN (Max)	2.822±0.149	0.765±0.005	0.588±0.004	0.289±0.016	0.373±0.012
	SGNN (FCMax)	3.114±0.114	0.735±0.009	0.554±0.008	0.278±0.021	0.364±0.017
	SGNN (Avg)	1.453±0.015	0.876±0.002	0.712±0.002	0.353±0.007	0.444±0.012
	SGNN (FCAvg)	1.658±0.067	0.857±0.007	0.689±0.008	0.305±0.018	0.399±0.021
	NGMN	1.191±0.048	0.904±0.003	0.749±0.005	0.465±0.011	0.538±0.007
	HGMN (Max)	1.210±0.020	0.900±0.002	0.743±0.003	0.461±0.012	0.534±0.009
	HGMN (FCMax)	1.205±0.039	0.904±0.002	0.749±0.003	0.457±0.014	0.532±0.016
	HGMN (BiLSTM)	1.169±0.036	0.905±0.002	0.751±0.003	0.456±0.019	0.539±0.018
LINUX 1000	SGNN (BiLSTM)	2.140±1.668	0.935±0.050	0.825±0.100	0.978±0.012	0.965±0.007
	SGNN (Max)	11.832±0.698	0.566±0.022	0.404±0.017	0.226±0.106	0.492±0.190
	SGNN (FCMax)	17.795±0.406	0.362±0.021	0.252±0.015	0.239±0.000	0.241±0.000
	SGNN (Avg)	2.343±0.453	0.933±0.012	0.790±0.017	0.778±0.048	0.811±0.050
	SGNN (FCAvg)	3.211±0.318	0.909±0.004	0.757±0.008	0.831±0.163	0.813±0.159
	NGMN	1.561±0.020	0.945±0.002	0.814±0.003	0.743±0.085	0.741±0.086
	HGMN (Max)	1.054±0.086	0.962±0.003	0.850±0.008	0.877±0.054	0.883±0.047
	HGMN (FCMax)	1.575±0.627	0.946±0.019	0.817±0.034	0.807±0.117	0.784±0.108
	HGMN (BiLSTM)	0.439±0.143	0.985±0.005	0.919±0.016	0.955±0.011	0.943±0.014

A.4 NGMN with different aggregation functions for both classification & regression tasks

We investigate the impact of different aggregation functions adopted by the aggregation layer of NGMN model for both classification and regression tasks. Following the default and same settings of previous experiments, we only change the aggregation layer of NGMN and use five possible aggregation functions: Max, FCMax, Avg, FCAvg, LSTM, and BiLSTM. As can be observed from Table 10 and Table 11, BiLSTM offers superior performance on all datasets for both classification

¹⁰<https://pytorch-geometric.readthedocs.io>

and regression tasks in terms of most evaluation metrics. Therefore, we take BiLSTM as the default aggregation function for NGMN, and fix it for the NGMN part in HGMM models.

Table 10: Classification results of NGMN models with different aggregation functions in term of AUC scores (%).

Model	FFmpeg			OpenSSL		
	[3, 200]	[20, 200]	[50, 200]	[3, 200]	[20, 200]	[50, 200]
NGMN (Max)	73.74±8.30	73.85±1.76	77.72±2.07	67.14±2.70	63.31±3.29	63.02±2.77
NGMN (FCMax)	97.28±0.08	96.61±0.17	96.65±0.30	95.37±0.19	96.08±0.48	95.90±0.73
NGMN (Avg)	85.92±1.07	83.29±4.49	85.52±1.42	80.10±4.59	70.81±3.41	66.94±4.33
NGMN (FCAvg)	95.93±0.21	73.90±0.70	94.22±0.06	93.38±0.80	94.52±1.16	94.71±0.86
NGMN (LSTM)	97.16±0.42	97.02±0.99	84.65±6.73	96.30±0.69	97.51±0.82	89.41±8.40
NGMN (BiLSTM)	97.73±0.11	98.29±0.21	96.81±0.96	96.56±0.12	97.60±0.29	92.89±1.31

Table 11: Regression results of NGMN models with different aggregation functions on **AIDS700** and **LINUX1000**.

Datasets	Model	$mse (10^{-3})$	ρ	τ	p@10	p@20
AIDS 700	NGMN (Max)	2.378±0.244	0.813±0.015	0.642±0.013	0.578±0.199	0.583±0.169
	NGMN (FCMax)	2.220±1.547	0.808±0.145	0.656±0.122	0.425±0.078	0.504±0.064
	NGMN (Avg)	1.524±0.161	0.880±0.010	0.717±0.012	0.408±0.044	0.474±0.027
	NGMN (FCAvg)	1.281±0.075	0.895±0.006	0.737±0.008	0.453±0.015	0.527±0.016
	NGMN (LSTM)	1.290±0.037	0.895±0.004	0.737±0.005	0.448±0.007	0.520±0.012
	NGMN (BiLSTM)	1.191±0.048	0.904±0.003	0.749±0.005	0.465±0.011	0.538±0.007
LINUX 1000	NGMN (Max)*	16.921±0.000	-	-	-	-
	NGMN (FCMax)	4.793±0.262	0.829±0.006	0.665±0.011	0.764±0.170	0.767±0.166
	NGMN (Avg)	4.050±0.594	0.888±0.008	0.719±0.012	0.501±0.093	0.536±0.112
	NGMN (FCAvg)	6.953±0.195	0.897±0.004	0.736±0.005	0.499±0.126	0.509±0.129
	NGMN (LSTM)	1.535±0.096	0.945±0.004	0.813±0.007	0.695±0.064	0.698±0.081
	NGMN (BiLSTM)	1.561±0.020	0.945±0.002	0.814±0.003	0.743±0.085	0.741±0.086

* As all duplicated experiments running on this setting do not converge in their training processes, their corresponding result metrics cannot be calculated.

A.5 NGMN with Different GNNs on regression tasks.

As a supplement to Table 6 in Section 4.3, Table 12 shows the experimental results of GCN versus GraphSAGE/GIN/GGNN in NGMN for the regression tasks.

Table 12: Regression results of different GNNs on **AIDS700** and **LINUX1000**.

Datasets	Model	$mse (10^{-3})$	ρ	τ	p@10	p@20
AIDS 700	NGMN-GCN (Our)	1.191±0.048	0.904±0.003	0.749±0.005	0.465±0.011	0.538±0.007
	NGMN-(GraphSAGE)	1.275±0.054	0.901±0.006	0.745±0.008	0.448±0.016	0.533±0.014
	NGMN-(GIN)	1.367±0.085	0.889±0.008	0.729±0.010	0.400±0.022	0.492±0.021
	NGMN-(GGNN)	1.870±0.082	0.871±0.004	0.706±0.005	0.388±0.015	0.457±0.017
LINUX 1000	NGMN-GCN (Our)	1.561±0.020	0.945±0.002	0.814±0.003	0.743±0.085	0.741±0.086
	NGMN-GraphSAGE	2.784±0.705	0.915±0.019	0.767±0.028	0.682±0.183	0.693±0.167
	NGMN-GIN	1.126±0.164	0.963±0.006	0.858±0.015	0.792±0.068	0.821±0.035
	NGMN-GGNN	2.068±0.991	0.938±0.028	0.815±0.055	0.628±0.189	0.654±0.176